



Research paper

The dynamic multi-box algorithm of atmospheric environmental capacity



Yunyan Jiang ^{a,b,1}, Jinyuan Xin ^{a,b,c,*1}, Zifa Wang ^{a,b}, Yongli Tian ^d, Guiqian Tang ^a, Yuanzhe Ren ^d, Lin Wu ^{a,b}, Xiaole Pan ^{a,b}, Ying Wang ^e, Danjie Jia ^{a,b}, Yongjing Ma ^a, Lili Wang ^a

^a State Key Laboratory of Atmospheric Boundary Layer Physics and Atmospheric Chemistry (LAPC), Institute of Atmospheric Physics, Chinese Academy of Sciences, Beijing 100029, China

^b University of Chinese Academy of Sciences, Beijing 100049, China

^c Collaborative Innovation Center on Forecast and Evaluation of Meteorological Disasters, Nanjing University of Information Science and Technology, Nanjing 210044, China

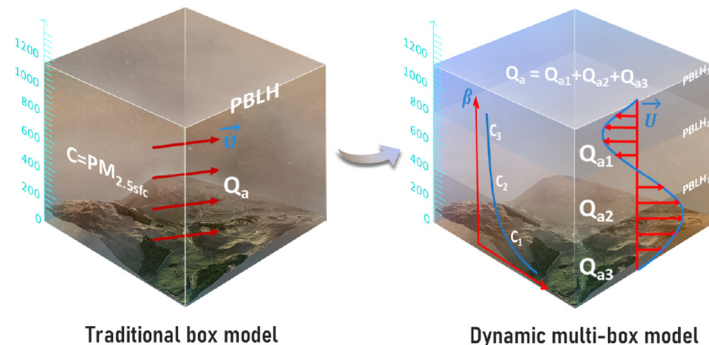
^d Inner Mongolia Autonomous Region environmental monitoring central station, Huhhot 010090, China

^e The College of Atmospheric Sciences, Lanzhou University, Lanzhou 730000, China

HIGHLIGHTS

- The dynamic multi-box algorithm accurately quantifies AEC for PM_{2.5} pollution control.
- The improvements for AEC of time coefficient and vertical multi-box are remarkable.
- For the first time synoptic circulation typing method is applied to AEC calculation.
- The residual AEC can indicate whether the atmosphere has been overloaded for PM_{2.5}.

GRAPHICAL ABSTRACT



ARTICLE INFO

Article history:

Received 19 September 2021

Received in revised form 30 September 2021

Accepted 9 October 2021

Available online 14 October 2021

Editor: Pingqing Fu

Keywords:

Atmospheric environmental capacity

Dynamic multi-box model

Synoptic circulation types

Regional pollution control

ABSTRACT

It is very important for air pollution prevention and control to accurately quantify atmospheric environment capacity (AEC) in the planetary boundary layer (PBL). This study developed a high temporal-resolution dynamic multi-box algorithm to estimate PM_{2.5} AEC with a PBL ceilometer and Doppler wind profile lidar in Beijing City. Compared with the traditional A-value method, two primary improvements are introducing the time coefficient and vertical multi-box assumption into the original box model. The algorithm can accurately calculate the PM_{2.5} AEC under different circulation patterns and predict the short-time dynamic change of AEC. The results show that the time coefficient effectively reduced the estimation errors when the initial PM_{2.5} concentration, horizontal wind speed and PBL heights change greatly with time, such situation is consistent with most circulation patterns. And the improvement of multi-box model is much more remarkable when the PM_{2.5} concentration and horizontal wind change greatly in the vertical direction, such as A, NE and W type circulations. The ideal AEC under polluted circulation patterns won't increase infinitely with wind speed and PBL height, generally less than 30 t/h. The horizontal advection has a much greater effect on expanding the capacity of PM_{2.5} than the vertical diffusion under clean circulation patterns, and the maximum value of ideal AEC can reach 50 t/h. The positive residual AEC under clean circulations indicates surplus capacity for PM_{2.5} because of vigorous turbulences, while weak diffusion and ventilation conditions under polluted circulations lead to negative residual AEC and insufficient capacity of atmosphere.

© 2021 Elsevier B.V. All rights reserved.

* Corresponding author at: #40 Huayanli, Chaoyang District, Beijing 100029, China.

E-mail address: xjy@mail.iap.ac.cn (J. Xin).

¹ These authors contributed equally to this work.

1. Introduction

In recent decades, with the frequent occurrences of severe pollution threatening to the environment and public health (Lin et al., 2010; Chen et al., 2019; Chen et al., 2020; Dai et al., 2021), the strategy of controlling single pollution source concentration has been unable to meet the requirements of harmonious development between social economy and environmental protection (Wang et al., 2014; Huang et al., 2021). Therefore, the strategy of controlling total volume of pollutants for improving the atmospheric environment was put forward in the 1990s. As the basis of total volume control, atmospheric environmental capacity (AEC) is the most important reference for scientific formulation of regional pollution discharge standards. At present, the principle methods for obtaining AEC include linear optimization method, multi-source model simulation method and A-value method (Xu et al., 2018b).

Linear programming method adopted the mathematical linear optimization theory to estimate AEC based on the associations between the diffusion of pollutants and the pollutants concentration at control points. That the pollutant concentration at control points satisfy the air quality standard is taken as the constraint and the maximum value of total emissions at different sources is taken as the objective, then the maximum allowable discharge or reduction amount at each source can be determined (An et al., 2004, 2007). Linear programming method can directly and reasonably allocate the total emissions (Lu and Shi, 2008). Xiao et al. (2008) adopted linear programming method to calculate the AEC of Tongzhou district, Beijing, pointing out that although the SO₂ emission in the whole district was far less than the AEC, it would still lead to heavy pollution in the areas where the emission sources were concentrated. Some researches (Qian and Wang, 2011; Wen et al., 2013) combined the advantages of linear programming method and other AEC calculation approaches so that the impacts of primary and secondary pollutants were taken into account and minimized the total cost of emission reduction. However, linear programming method depends on too many factors, including topography, meteorological conditions, types of pollutant discharged and total amount of emissions and so on. Furthermore, linear programming method cannot be applied to nonlinear processes as well, that is, it is not applicable for the secondary chemical reactions pollutants. With the continuous improvements of advanced air quality models such as WRF-Chem, CMAQ and CAMx, they are fully capable to simulate the coupled physical and chemical processes, becoming a useful tool for revealing the evolution law and internal mechanism of the pollution events (Xue et al., 2013b). Li et al. (2010) used the CMAQ model to simulate the AEC of various pollutants under different air quality guideline-satisfaction ratio, and discussed the seasonal characteristics of AEC. Xue et al. (2014a, 2014b) designed an iterative reduction of source emissions algorithm to estimate AEC using the CAMx model under the conditions that PM_{2.5} concentration satisfied the air quality criteria, and further investigated the pattern of regional transport of PM_{2.5} and its chemical components. In recent years, AEC has been studied in many aspects taking advantage of the same iterative approach based on various air quality models, such as Geos-Chem, WRF-CAMx, WRF-Chem, CAMx-PSAT (Xue et al., 2013a; Hao et al., 2017; Li et al., 2018; Yang et al., 2019; Xu et al., 2019; Gao et al., 2021). The influential mechanisms of source emissions, meteorological factors, large-scale circulation patterns, summer monsoon and different stages of economic development on AEC were further revealed. Numerical simulation method takes the effects of physical and chemical processes on the AEC into account, but the calculation is complicated and requires a lot of computing resources. In addition, the investigation and arrangement of emission source inventory has great uncertainty, and it cannot be used to simulate dynamic AEC due to weak timeliness.

The A-value method was derived from the primitive equation of box model based on the laws of dilution and diffusion of atmospheric pollutants. Taking the air quality standard as the control target, the maximum source discharge determined by A-value approach is the AEC of control region. Xu and Zhu (1989) simplified the box model equation under

long time equilibrium conditions, adding dry deposition, wet deposition and chemical decay terms into the equation and developing it into the current A-value approach. In A-value method, AEC of a specific control area and specific pollutant only depends on the coefficient A. Therefore, this method used to calculate AEC is called A-value method. In the national standard, the coefficient A is set to a series of empirical constant values with reference to the meteorological conditions of the base year in different climate regions (Xu et al., 1990; Xu and Li, 1993). Some subsequent studies calculated the coefficient A by planetary boundary layer (PBL) heights determined by stability grading and wind speed profiles determined by logarithmic law (Wang and Pan, 2005; Ou, 2008; Wang et al., 2015). Han et al. (2017) used A-value approach in the regional climate model Regional Climate Model (RegCM4) to predict PM_{2.5} AEC in main economic zones of China and haze pollution potential in 21st century. A-value method has strong operability and its formula is concise with clear physical meaning. In addition, the changes in the temporal and spatial layout of emission sources does not affect AEC directly because the box model assumes that the pollution sources within the control region are uniformly distributed plane sources (Hanna et al., 1982). Therefore, it becomes the most widely used calculation approach of AEC (Yuan et al., 1996; Wang et al., 1997; Xu et al., 2016, 2018a).

Nevertheless, the hypothesis that the pollution concentration is uniform in the box is unreasonable for aerosols, and the simplification of box model equation is under the long time equilibrium conditions. Therefore, the current A-value method is only available for annual AEC of gaseous pollutants. Given that there are still some unreasonable assumptions and deficiencies in practical application of the current A-value method, this paper aims to improve the A-value algorithm using the high temporal resolution PBL observation data detected from ceilometer and Doppler wind profile lidar. The evolution characteristics of AEC under different PBL structures and circulation patterns were further revealed. The rest of the paper is arranged as follows. Section 2 describes the data and weather circulation typing methods used in this paper. Section 3 introduces the creation of dynamic AEC in detail. Section 4 compares the improved dynamic AEC with AEC derived from A-value and further reveals the evolution characteristics of dynamic AEC under different circulation patterns and PBL structures.

2. Data and method

Beijing is located in the North China Plain (NCP) with the Taihang Mountain located in the west and the Yan Mountain located in the north, the topography decreases gradually from northwest to southeast. Due to the complex terrain, the PBL structure on different underlying surfaces varies greatly. Furthermore, an urban area contains thousands of individual emission sources. The application of a diffusion model to each of these sources is impractical. Consequently we assume that emissions from the ground surface are uniform over that particular area (Hanna et al., 1982), in this way can AEC of the area be calculated in one box based on the assumption of the box model. Meanwhile, the studied areas will be divided by administrative region for future practical application according to current national emission standards. Therefore, six districts including Haidian, Chaoyang, Dongcheng, Xicheng, Shijingshan and Fengtai (Fig. 1), which are located in the plain areas of Beijing, were selected to develop a dynamic multi-box AEC algorithm for PM_{2.5} and further study the evolution characteristics of AEC under different PBL structures and circulation patterns. These six districts are assumed to have similar terrain, meteorological conditions and PBL structure in the study, and the emissions in each district are treated as a uniform plane source.

2.1. Fine-resolution aerosol and wind data in the vertical direction

The PBL field observation experiment based on ceilometer and Doppler Wind Profile Lidar was conducted from January 2018 to

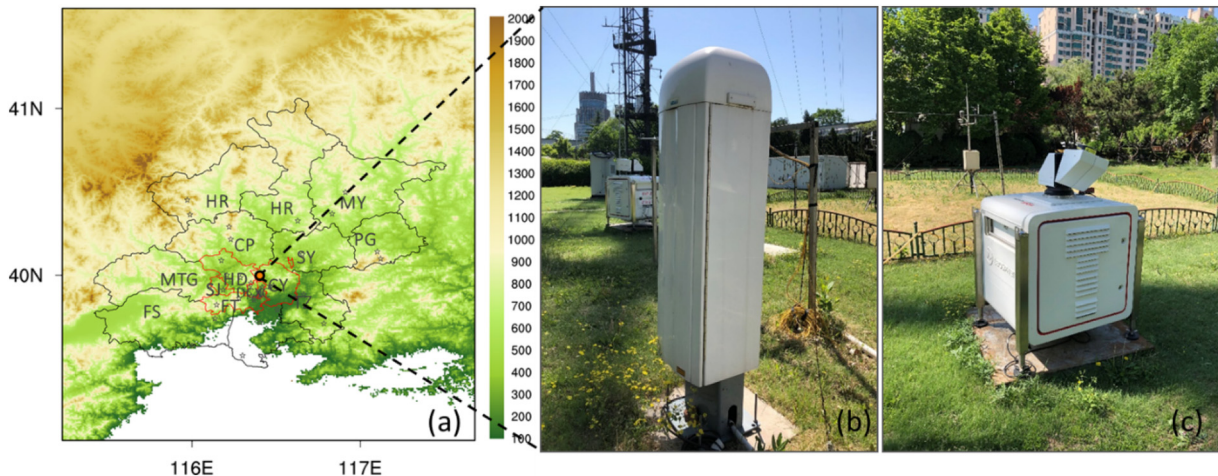


Fig. 1. The terrain height of Beijing city (shaded; units: m) (a). The gray stars indicate the locations of air quality monitoring sites in Beijing. The control area for dynamic AEC (in red) includes Dongcheng (DC), Xicheng (XD), Chaoyang (CY), Haidian (HD), Fengtai (FT) and Shijingshan (SJ) districts in Beijing. Ceilometer (b) and Doppler wind profile lidar (c) used in this paper.

December 2019 in the courtyard of the Institute of Atmospheric Physics (39.6°N and 116.2°E), Chinese Academy of Sciences, Beijing (Fig. 1) (Jiang et al., 2021a,b). The Vaisala CL51 ceilometer uses light detection and ranging (lidar) technology to measure the backscatter caused by haze, fog, precipitation and clouds, detecting the cloud base height while generating backscatter profiles (Tang et al., 2015, 2016). The vertical resolution of backscatter coefficient profile is 10 m, and the maximum detection range can reach 7.7 km. The temporal resolution is set to 16 s for the measurements of backscatter coefficient (Tang et al., 2015, 2016). Nevertheless, the PBLH (planetary boundary layer height) is calculated every 10 min because of temporal sliding averages to filter out unwanted fluctuations. Based on the assumption that the aerosol concentration in one aerosol layer is close to the constant value and significantly higher than that in the free atmosphere (Steyn et al., 1999), aerosol layers are separated by the minima of the local backscatter gradient with BL-VIEW software of ceilometer. The first three largest negative gradients in the backscatter profile are identified as the PBLHs of different aerosol layers. Its enhanced optics and electronics enables the ceilometer to detect fine boundary-layer structures whose counterparts are seen in temperature profile (Münkel et al., 2007). Therefore, the pollutants inside the PBL are divided into different box vertically by using backscattering profiles. Windcube 100S scanning Doppler lidar is an active remote sensing device based on lidar technology. The Doppler shift of the backscattering of detected atmospheric particulate matter (aerosols, dust, water droplets, etc.) is used to derive the three-dimensional wind fields. The Doppler lidar has four scanning modes. In this paper, the DBS scanning mode is chosen to detect the wind profiles. The DBS (Doppler beam-swinging technique) mode includes four LOSs (lines of sight) spaced 90° apart with a fixed elevation angle and one vertical LOS. Data with a carrier-to-noise ratio (CNR) lower than -27 dB will be discarded. The vertical detection range of the wind profile is from 50 m to 3300 m, with a vertical resolution of 25 m and a temporal resolution of 20 s (Jiang et al., 2021a,b).

2.2. PM_{2.5} data

The hourly PM_{2.5} concentrations are obtained from the National Urban Air Quality Real-time Publishing Platform (<http://106.37.208.233:20035/>) issued by the Ministry of Ecology and Environment. The 35 air quality monitoring stations in Beijing are shown in Fig. 1. The hourly PM_{2.5} concentrations at these stations were used to categorize synoptic circulations into clean types and polluted types. Hourly PM_{2.5} concentrations of 17 monitoring stations in Haidian,

Chaoyang, Dongcheng, Xicheng, Shijingshan and Fengtai districts were used to calculate dynamic AEC.

2.3. Circulation typing and meteorological data

The Lamb-Jenkinson weather typing (LWT) approach is a half objective circulation classification technique (Lamb and Hh, 1972) using empirical rules (Jenkinson and Collison, 1977; Trigo and DaCamara, 2000). Daily mean sea level pressure (MSLP) at point-grids centered on Beijing city (Jiang et al., 2021a) were used to calculate the direction and vorticity of geostrophic wind, and each day can be categorized into one certain type of the predefined 26 types. It's widely adopted in large-scale circulation categorization because of its automation and explicit meteorologically meaning (Russo et al., 2014; Pleijel et al., 2016; Liao et al., 2017). The 26 predefined weather types include two rotational types (cyclonic, C; anticyclonic, A), eight directional types (northeasterly, NE; easterly, E; southeasterly, SE; southerly, S; southwesterly, SW; westerly, W; northwesterly, NW; and northerly, N), and sixteen hybrid types (CN, CNE, CE, CSE, CS, CSW, CW, CNW, AN, ANE, AE, ASE, AS, ASW, AW, and ANW). The typical cases with the same circulation pattern maintained for two consecutive days were selected to study dynamic AEC characteristics of PM_{2.5} under different circulation patterns, based on two primary criteria. First, both ceilometer and Doppler lidar must be ensured to measure continuously during typical case processes. Second, the circulation type varies day-by-day generally, one specific type maintaining for two consecutive days is assumed to be sufficiently typical to represent this circulation pattern. The daily mean sea level pressure (MSLP) and wind fields at 850 hPa from the National Center for Atmospheric Research (NCAR) reanalysis data (gridded at 2.5° × 2.5°) were used to classify the synoptic circulation patterns and depict the background circulations of the typical circulation types.

3. Dynamic atmospheric environmental capacity

According to national standards, a series of empirical values of the base year in different climate regions are adopted to represent the coefficient A in traditional A-value algorithm. However, such empirical setting will lead to considerable uncertainties of AEC. Therefore, AEC is calculated from fine-resolution observational data in this study rather than using empirical regional coefficient A.

$$\frac{\partial C}{\partial t} LH = Lq_a + UH(C_b - C) + L \frac{\partial H}{\partial t} (C_a - C) \quad (1)$$

$$Q_a = q_a S = AC_s \sqrt{S} \quad (2)$$

The box model can be expressed by Eq. (1) (Hanna et al., 1982), where C is the pollutant concentration, L is the length of the control area, H is represented by the height of PBL, q_a is pollutant emission per unit time and per unit area, U is the average wind speed inside the control region, C_b and C_a is the concentration upwind of the city and above the PBL height, respectively. The A-value method assumes that the box model is in a long-term equilibrium state and the pollutants in the box are uniformly distributed, that is $\frac{\partial C}{\partial t} = \frac{\partial H}{\partial t} = 0$ and $C = \frac{L}{H} \frac{q_a}{U}$. Then the simplified solution of AEC can be easily described as Eq. (2), in which S is the area of control region, Q_a , namely AEC, is the maximum allowable discharge per unit time when the pollution concentration is equal to the standard concentration C_s . The formula 2 is the so-called A-value method, and the traditional way take the easiest calculation to set the coefficient A to a series of constant values according to the climatic regions. When the effects of pollutants dry and wet deposition on AEC are considered, the coefficient $A = \frac{\sqrt{\pi}UH}{2} + (V_d + V_w)\sqrt{S}$, otherwise $A = \sqrt{\pi}UH/2$, where V_d is the dry deposition rate acquired from the ratio of deposition flux to pollution concentration, and V_w is the wet deposition rate denoting the impacts of precipitation cleaning (Xu et al., 2018a).

$$\frac{\partial C}{\partial t^*} = C^* - C \quad (3)$$

$$q_a = (C - C_0 e^{-t^*})HU/L \quad (4)$$

$$Q_a = q_a S = (C - C_0 e^{-t^*})HU\sqrt{\pi S}/2 \quad (5)$$

$$h_1 = PBLH_1; h_2 = PBLH_2 - PBLH_1; h_3 = PBLH_3 - PBLH_2 \quad (6)$$

$$C_1 = C_s; C_2 = C_1 * \frac{\int_{PBLH_1}^{PBLH_2} \beta dh}{\int_0^{PBLH_1} \beta dh} * \frac{h_1}{h_2}; C_3 = C_1 * \frac{\int_{PBLH_2}^{PBLH_3} \beta dh}{\int_0^{PBLH_1} \beta dh} * \frac{h_1}{h_3} \quad (7)$$

$$U_1 = \frac{\int_0^{PBLH_1} \bar{U} dh}{h_1}; U_2 = \frac{\int_{PBLH_1}^{PBLH_2} \bar{U} dh}{h_2}; U_3 = \frac{\int_{PBLH_2}^{PBLH_3} \bar{U} dh}{h_3} \quad (8)$$

$$Q_a = Q_{a1} + Q_{a2} + Q_{a3} \quad (9)$$

The box is assumed to reach equilibrium state after long-term adjustment and the pollutants concentration won't change in A-value method. Therefore, Eq. (2) is just suitable for long time scale estimation, only annual AEC can be calculated. However, the real meteorological conditions are constantly changing, and the AEC is dynamic actually. A long time scale AEC is not conducive to the allocation of pollutant emission and is of little significance in practical use because the layout of pollution sources and the way of emission in many cities are constantly changing. By contrast, dynamic AEC can realize real-time prediction of AEC in severe pollution events and provide real-time guarantee for environmental planning and scientific decision-making, it is of great significance to increase the temporal resolution of AEC. In order to obtain the dynamic hourly-AEC, the dimensionless time scale $t^* = \frac{tU}{L}$ is defined based on the original equation (Eq. (1)) of the box model (Lettau, 1970). Then the pollution concentration can be described as Eq. (3), in which t^* is defined as the flushing time required for the air to pass completely over the urban area, $C^* = \frac{L}{H} \frac{q_a}{U}$ is the pollutants concentration in equilibrium state (Lettau, 1970; Hanna et al., 1982). It should be noted that, when calculating hourly-AEC, the length of control regions should be kept within the scale of airflow scouring within 1 h. Therefore, a district-scale control region was selected in this paper to study the characteristics of dynamic AEC and the impacts of synoptic circulations on it. Take the solution of partial differential Eq. (3) ($C = C^* + (C_0 - C^*)e^{-t^*}$) into the original Eq. (1), then the pollutant emission per unit time is expressed by formula 4, where C_0 is the pollutant concentration at the

initial time. Assuming that the control area is approximately circular and L is taken as the equivalent radius ($L = 2\sqrt{S/\pi}$), then the dynamic AEC is Eq. (5). Compared with AEC calculated by A-value, $C_0 e^{-t^*}$ is the time coefficient term, denoting the effects caused by the initial concentration changing with time on AEC. The time coefficient term is trivial and is allowed to be omitted when calculating annual AEC, while it cannot be negligible when calculating hourly-AEC. Compared with horizontal advection and emission, the deposition and chemical decay of pollutants within 1 h are negligible when calculating the dynamic AEC, which are not considered in this article.

In the real atmosphere, the aerosol inside the PBL has obvious stratified structure, and the PBL structure is significantly different under various circulations (Jiang et al., 2021a, 2021b). However, A-value method simply assumes that the pollutants are uniformly distributed in the box. Such assumption is approximately valid for gaseous pollutants but will lead to considerable errors of AEC of aerosol pollutants. Further improvement is made based on the dynamic AEC to minimize the errors caused by aerosol stratification. The multi-aerosol-layer structure within PBL suggests that the multi-box model should be designed in the vertical direction to make it suitable for calculating the AEC of PM_{2.5}. The heights of different boxes were calculated respectively using formula 6 based on the PBL heights retrieved by the local minimum gradient of backscatter profiles. Supposing that the pollutants in each aerosol layer are uniformly dispersed, and the ratio of the integrated backscatter coefficient is taken as the ratio of the concentration of different boxes. Therefore, the PM_{2.5} concentration in the upper box can be obtained by combining with the observed concentration (Eq. (7)). C_s is the observed concentration of PM_{2.5} in the surface layer, and β is the backscatter coefficient at the corresponding time. The average wind speed of different boxes can be solved by formula 8, where \bar{U} is the horizontal wind speed profile. Bring Eqs. (6), (7) and (8) into the dynamic AEC (Eq. (5)), and the AEC from the bottom box to the top one is Q_{a1} , Q_{a2} and Q_{a3} , respectively. Finally, the dynamic multi-box AEC at the corresponding time can be obtained by adding AEC together (Eq. (9)).

According to Ambient Air Quality Standards of China (GB 3095-2012, 2012), the 24-hour averaged concentration limits for PM_{2.5} has two levels. The first level is 35 µg/m³ and the second level is 75 µg/m³. We adopted stricter emission standard 75 µg/m³ as a criterion when calculating AEC with A-value method (Han et al., 2017). The AEC represents the maximum allowable emission intensity when the pollutants concentration meets the air quality standard, which is an ideal AEC. This article widens the concept of ideal AEC and the AEC is called actual AEC when the PM_{2.5} concentration is set to the real concentration, indicating the actual pollution emission intensity inside the PBL. Furthermore, the difference between the ideal AEC and the actual AEC is called residual AEC, which stands for the pollution emission that can be increased (or already overloaded) under the certain atmospheric conditions and PBL structure. The evolutionary characteristics of these three types AEC under the background of different synoptic circulations will be discussed in detail later.

4. Results and discussions

4.1. Circulations classification and planetary boundary layer structure

The results of Lamb-Jenkinson circulations classification are shown in Fig. 2. The first ten circulation patterns, including two vorticity types (C, A) and eight directional types (NE, E, SE, S, SW, W, NW, N), accounted for more than 75% of the total occurrence frequencies. The vorticity and directional types were more representative because the hybrid types had the mixed characteristics of them. Therefore, this article chose the first ten circulations as the typical types to conduct the subsequent research (Pope et al., 2016; Liao et al., 2017). Based on the daily average PM_{2.5} concentration, circulations with concentration less

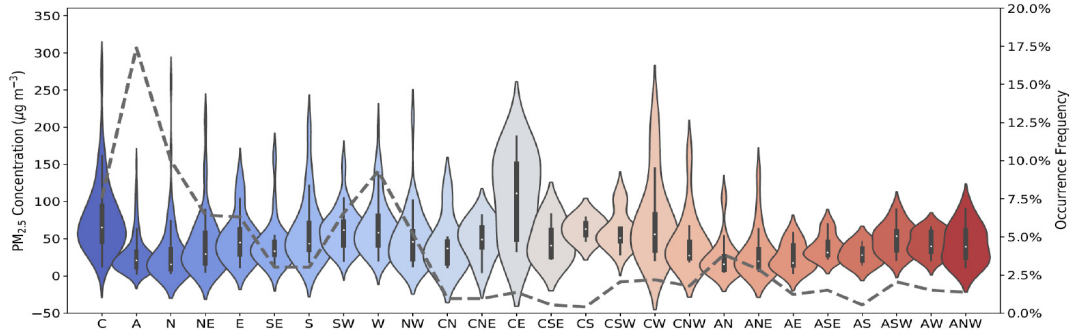


Fig. 2. Daily average PM_{2.5} concentration of Beijing (box plots; units: $10^{-1} \mu\text{gm}^{-3}$) and the occurrence frequencies of 26 weather types (dashed lines) from 2018 to 2019.

than $50 \mu\text{g/m}^3$ were further defined as clean types, while circulations with concentration greater than $50 \mu\text{g/m}^3$ were defined as polluted types. The clean circulations included A, N, NE, SE and NW patterns, and the average daily PM_{2.5} concentration was $28 \mu\text{g/m}^3$, $30 \mu\text{g/m}^3$, $42 \mu\text{g/m}^3$, $43 \mu\text{g/m}^3$ and $49 \mu\text{g/m}^3$, respectively. Clean types accounted for 42% of total circulations, in which the anticyclonic (A) type was much more than other circulation types, accounting for 18%. While the polluted circulations included C, W, SW, S and E patterns, and the average daily PM_{2.5} concentration was $77 \mu\text{g/m}^3$, $66 \mu\text{g/m}^3$, $62 \mu\text{g/m}^3$, $60 \mu\text{g/m}^3$ and $51 \mu\text{g/m}^3$, respectively. Polluted types accounted for 34% of the total circulations, in which the westerly (W) type was much more than other circulation types, accounting for 10%.

Different clean circulations were at different stages of the eastward and southward movements of the high pressure which was located in the northern or northwestern region of the NCP (Fig. 3a–e). When the high pressure center was located in Beijing (Fig. 3a), the A-type circulation had the most strengthened purifying intensity. In the N-type circulation, Beijing was located in the periphery of high pressure and far away from the main body of high pressure (Fig. 3b). However, strong northerly winds had already developed to NCP, therefore, the cleaning strength was second to A-types. Both the prevailing weak northerly

winds under NE-type circulation (Fig. 3c) and southerly winds under SE-type circulation (Fig. 3d) lead to much weaker purification than the first two kinds patterns. The high pressure circulation was very weak in NW-type circulation, and Beijing was located in the westerly zone at the bottom of the low pressure (Fig. 3e). In the polluted circulations C, W and SW types, the NCP region was significantly affected by the low pressure system. The anticyclonic circulation over the sea was strong, and the prevailing wind was southerly wind in the lower troposphere. In the C-type circulation, Beijing was located in the low pressure center. That the southerly winds transported pollutants from eastern China to the north and converged with the westerly winds was highly favorable for the aggravation and accumulation of pollution in Beijing (Fig. 3f). While in the W and SW circulations, Beijing was located at the bottom of the low pressure and the southerly winds speed was notably higher than that in C-type (Fig. 3g, h). Strong wind was beneficial to the transport of pollutants in the early stage but unfavorable to the long-term accumulation of pollutants (Jiang et al., 2021a). In the S-type circulation, the southerly winds in the rear of high pressure carried low concentration of pollutants from the sea (Fig. 3i). However in the E-type circulation, the northerly winds prevailed in Beijing, which was adverse to the development of pollution and the PM_{2.5} concentration was the

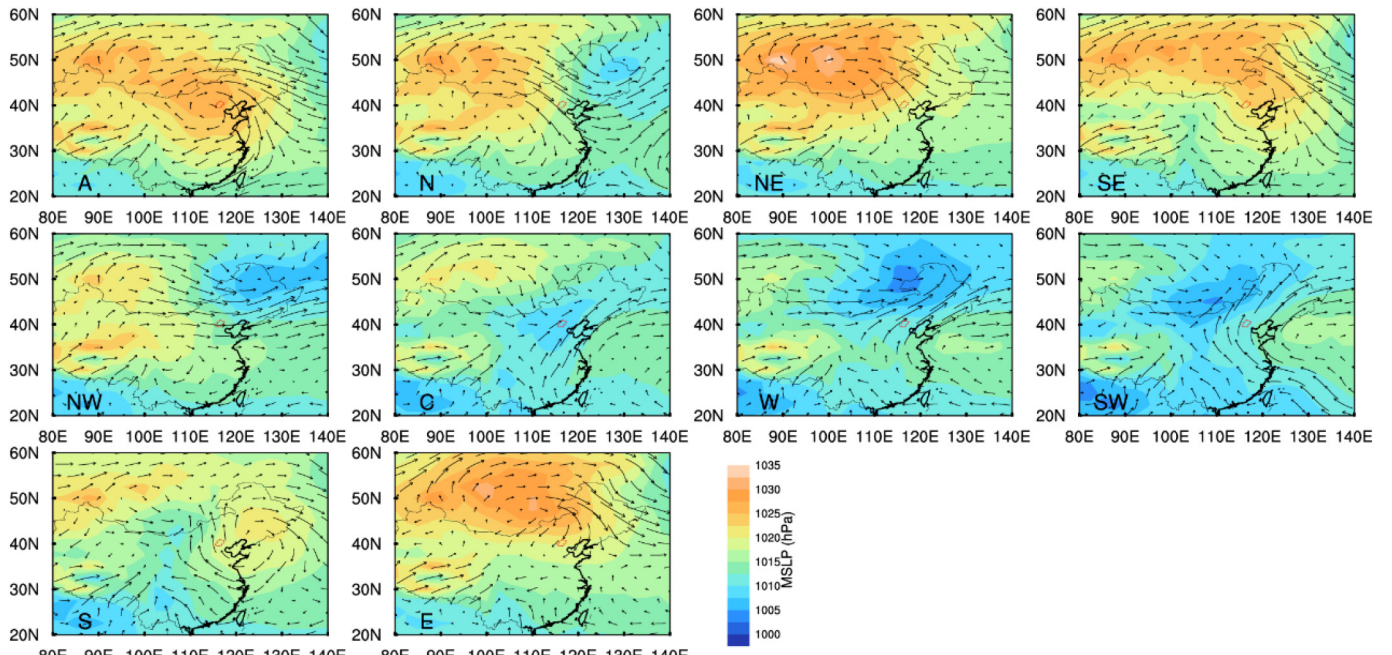


Fig. 3. The daily MSLP (mean sea level pressure) (shaded; units: hPa) and wind fields at 925 hPa (vectors; units: ms^{-1}) for different circulation patterns from 2018 to 2019. Clean types include anticyclonic (A), northerly (N), northeasterly (NE), southeasterly (SE) and northwesterly (NW) circulations. Polluted types include cyclonic (C), westerly (W), southwesterly (SW), southerly (S) and easterly (E) circulations.

lowest among all polluted types (Fig. 3j). NW and E circulations were the transitional circulations between clean and polluted types, whose characteristics of purifying and polluting capacities were not remarkable.

In most circumstances, there were multiple aerosol layers inside the PBL and the aerosol concentration varies observably between different layers (Fig. 4). In the clean circulations with strong purification, the air was very clean and the aerosol concentration was very low (Fig. 4a, b). Strong northwest winds from the upper layer penetrated into the PBL so that the PBL height changed little. The lower aerosol layer in A-type circulation was about 500 m and the higher one ranged from 1000 m to 2000 m (Fig. 4a). While there was only one aerosol layer in N-type circulation, whose height was lower than 500 m (Fig. 4b). The predominant winds were northeast winds inside the PBL under the background of NE-type circulation, and the atmospheric purification capacity was slightly smaller than A and N patterns (Fig. 4c). The diurnal variation of the PBL height in under SE and NW circulations with weak purification capacity was obvious, and the maximum value can reach 2000 m. There were not consistent northerly winds inside the PBL, and weak pollution occurred along with southerly winds (Fig. 4d, e). The PBL, whose height was generally lower than 1500 m, were all multi-aerosol layers structure under the polluted circulations. There were three aerosols layers without diurnal variations under the C type circulation (Fig. 4f). The PBL structures under W, SW and S pattern circulations were similar, which was characterized by residual boundary layer overlying on the stable boundary layer at night (Fig. 4g, h and i). The stable boundary layer rose gradually and merged with the residual layer after sunrise, while it rapidly collapsed into two layers within 2–3 h after sunset (Jiang et al., 2021b). In the nighttime, the northerly mountain breezes generated by the thermal contrast between the mountain and the valley coupled with the environmental southerly winds in the horizontal and vertical directions, respectively, leading to a temperature inversion and a convergent area of severe pollution

consequently (Jiang et al., 2021a). Differed from other polluted circulations, strong northerly winds prevailed above the PBL while weak southerly winds prevailed inside the PBL under the E-type circulation. The multi-aerosol layers were not explicit and the PBL height varied little (Fig. 4j).

4.2. Dynamic atmospheric environmental capacity (AEC) and algorithm evaluation

As indicated above, the vertical distribution of aerosols, PBL heights and horizontal wind speed under different circulations varied greatly, resulting in significant differences in AEC. Therefore, we calculated the actual AEC of six districts in Beijing by applying dynamic AEC algorithm, and then compared the dynamic AEC with AEC without time coefficient (Fig. 5a, d), AEC without multi-box improvements (Fig. 5b, e) and AEC calculated by A-value without any improvements (Fig. 5c, f), respectively. Because the influences of initial pollution concentration were neglected in the A-value method (Fig. 5a, d), the AEC calculated by the old algorithm was much greater than the dynamic AEC calculated with time coefficient. We can also drew the same conclusion from the comparison between formula 2 and formula 5 that the improvement of adding initial concentration changing with time was necessary for hourly AEC otherwise it will result in overestimation of AEC. In addition, taking the observed PM_{2.5} concentration as the concentration of homogeneous pollution in the single-box model will also contribute to overestimation of AEC (Fig. 5b, e) because the PM_{2.5} concentration usually decreased from the surface to the PBL top. Therefore, the vertical multi-box model effectively reduced the errors caused by the vertical variations of aerosols concentration. Hourly AEC under clean circulations was generally less than 40 t/h, the improvements of old A-value algorithm were the most distinctively under NE and SE circulations (Fig. 5c). When AEC was less than 20 t/h, the standard deviation of the old A-value algorithm increased linearly, while the standard deviation

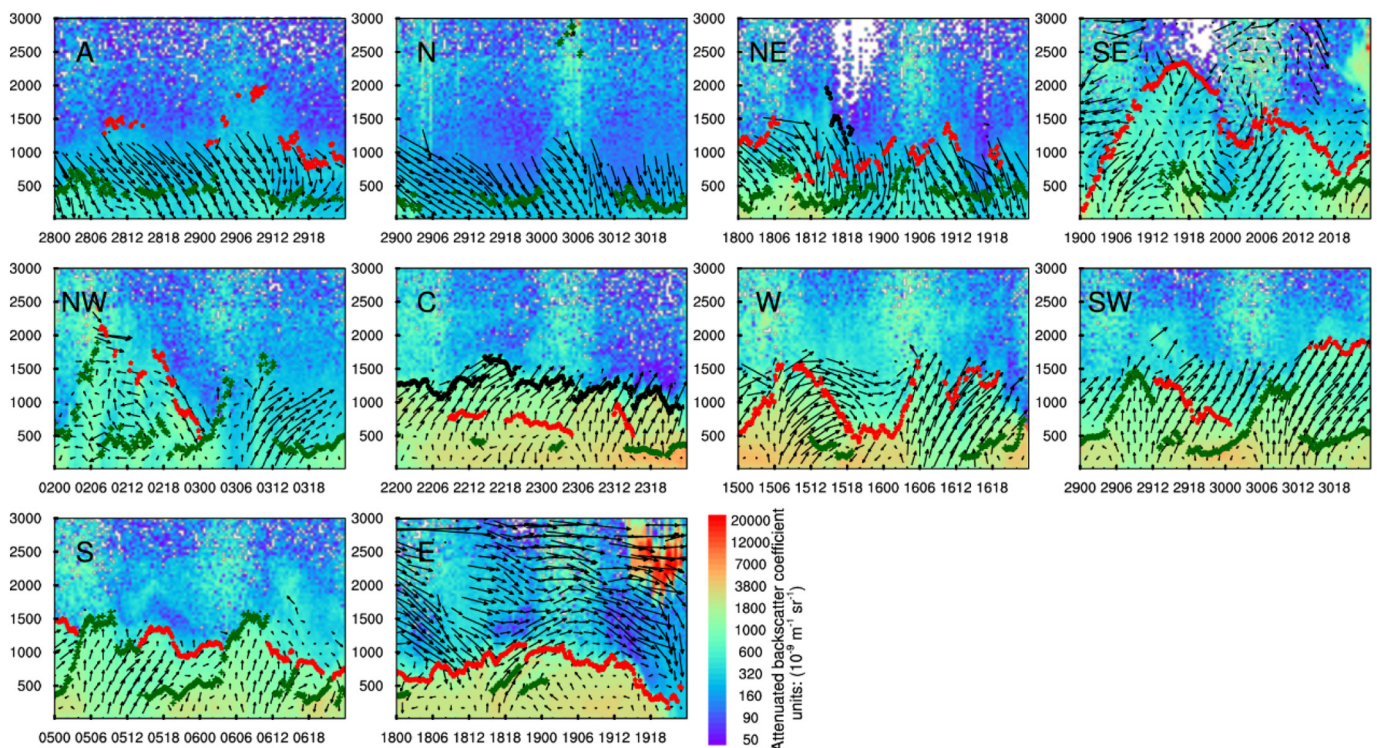


Fig. 4. Attenuated backscatter coefficient (shaded; units: $10^{-9} \text{ m}^{-1} \text{ sr}^{-1}$) and horizontal winds (vectors; units: ms^{-1}) for different circulation patterns. The green crosses, red stars, and black hollow dots represent the lowest, middle, and top PBLH, respectively. Clean types include anticyclonic (A), northerly (N), northeasterly (NE), southeasterly (SE) and northwesterly (NW) circulations. Polluted types include cyclonic (C), westerly (W), southwesterly (SW), southerly (S) and easterly (E) circulations.

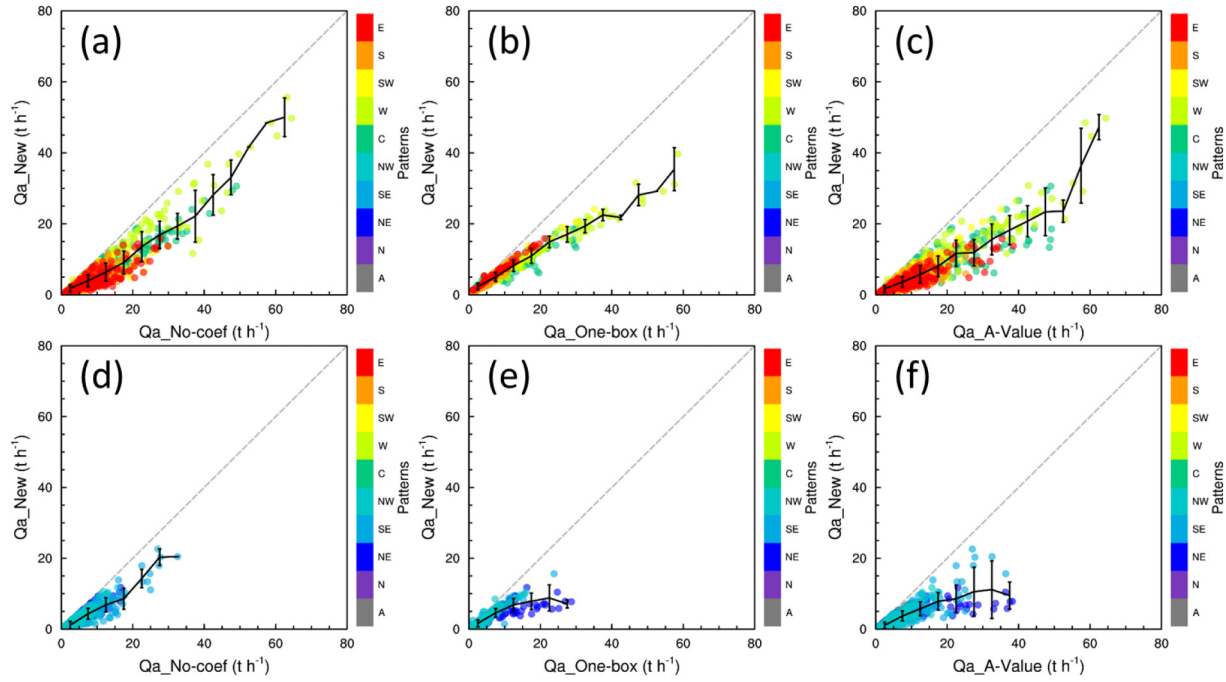


Fig. 5. Comparison of new AEC calculated by improved algorithm (Q_a_{New}) and AEC without time coefficient ($Q_a_{\text{No-coef}}$) (a, d), AEC without vertical multi-box improvement ($Q_a_{\text{One-box}}$) (b, e) and AEC calculated by A-value algorithm ($Q_a_{\text{A-Value}}$) (c, f) under clean patterns (a, b, c) and polluted circulation patterns (d, e, f). The error bars indicate standard deviation of new AEC.

increased more rapidly and no longer kept linearly when AEC was greater than 20 t/h. The AECs under polluted patterns were obviously higher than that under clean patterns, but generally less than 80 t/h (Fig. 5f). When the AECs under polluted types were less than 50 t/h, the standard deviation of the old A-value algorithm generally increased linearly with AEC.

In order to further quantify the AEC error caused by the A-value algorithm, the root-mean-square error (RMSE) of AEC without time coefficient, AEC without multi-box improvements and AEC retrieved by old

A-value algorithm were calculated respectively (Fig. 6). The average RMSE under clean types was 3.4 t/h (Fig. 6a). The RMSE of AEC without time coefficient and AEC without multi-box assumption was 1.0 t/h and 1.5 t/h, respectively under A-type circulation. The PBL was characterized by single aerosol layer under N-type circulation, and the RMSE was completely caused by lack of time coefficient. $\text{PM}_{2.5}$ concentration was very low, the RMSE was only 0.2 t/h. The RMSE of NE-type was 7 t/h, which was obviously larger than that under the first two circulations. Unlike other clean types, $\text{PM}_{2.5}$ concentration in the lower layer was

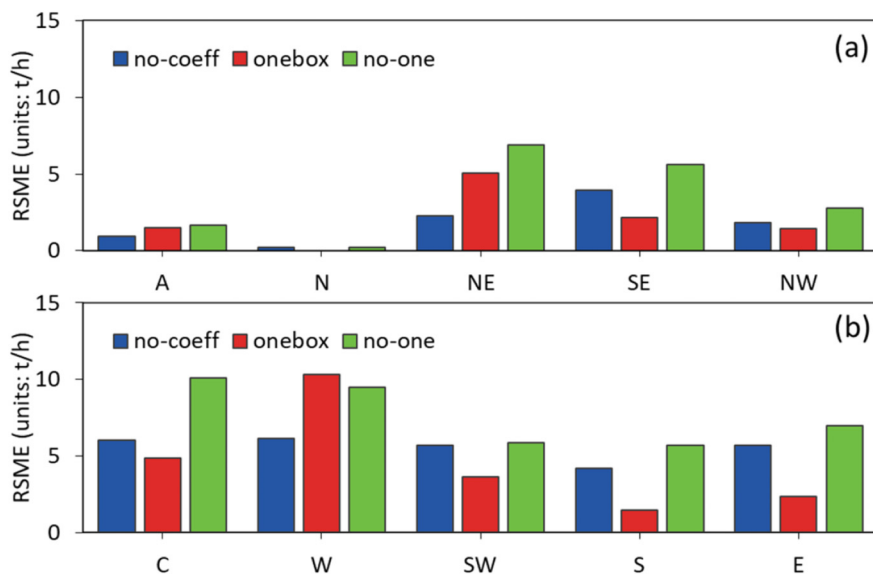


Fig. 6. The RMSE (root-mean-square error) between new AEC calculated by improved algorithm and AEC without time coefficient (no-coeff), AEC without vertical multi-box improvement (onebox) and AEC calculated by A-value algorithm (no-one), respectively under clean patterns (a) and polluted circulation patterns (b). Clean types include anticyclonic (A), northerly (N), northeasterly (NE), southeasterly (SE) and northwesterly (NW) circulations. Polluted types include cyclonic (C), westerly (W), southwesterly (SW), southerly (S) and easterly (E) circulations.

much higher than that in the upper layer under NE-type circulation (Fig. 4c). RMSE caused by single-box model was evidently greater than that caused by lack of time coefficient. The RMSE of AEC derived from old A-value method under SE and NW type circulations was 5.6 t/h and 2.7 t/h, respectively. The RMSE of AEC under polluted types was distinctly greater than that under clean types, with an average of 7.6 t/h (Fig. 6b). The RMSE of AEC derived from old A-value method was about 10 t/h under C and W circulations which were the most favorable types for pollution. The absence of time coefficient had a far greater impact on AEC under C-type circulation while the situation was opposite under W-type circulation due to the much higher concentration PM_{2.5} near the surface than that in the upper layer. The RMSE under SW, S and E type circulations were close to each other. It was 4–6 t/h without time coefficient and was 1.5–3.5 t/h without vertical multi-box improvement.

4.3. Actual AEC, ideal AEC and residual AEC under different circulations

The study further investigated the ideal and actual capacity of pollutants under different circulations and PBL structures to quantitatively predict the residual or exceeded capacity of the atmosphere. The diurnal variation characteristics of three kinds of AECs are shown in Fig. 7. The PM_{2.5} concentration was low under clean types, the actual AECs were obviously less than that under polluted types. The A, N and NE types were characterized by large wind speed inside the PBL and the PBL heights varied little (Fig. 4) so that the AECs were relatively small and showed no obvious diurnal variations (Fig. 7a). While under the SE

and NW circulations, the AEC showed the same diurnal variation characteristics with the PBL heights (Fig. 7a, c, e). The daily maximum value of AEC appeared around 15:00 to 16:00 (local time, hereinafter) with vigorously developed turbulences and high PBL height. The ideal AECs of clean types (Fig. 7c) were much higher than the actual AEC (Fig. 7a) so that the residual AECs were all positive (Fig. 7e), which meant there was still room for more PM_{2.5} under the meteorological conditions at the time. The ideal AEC under A-type circulation varied greatly from day to night, with the average value greater than 10 t/h in the daytime while less than 10 t/h at night (Fig. 7c). The residual AEC was 10–20 t/h in the daytime, and the maximum value can reach more than 40 t/h (Fig. 7e). Therefore, under the condition of favorable diffusion height and ventilation caused by high PBL height and strong winds, PM_{2.5} emission intensity can be increased by 40 tons per hour to the maximum. Nevertheless, the residual AEC at night was 5–15 t/h and notably less than that in the daytime (Fig. 7e). The residual AEC under N-type circulation was approximately equal to the ideal AEC due to the low PM_{2.5} concentration and small actual AEC. The ideal AEC under NE-type circulation was second to A type, the maximum was frequently larger than 30 t/h and the average residual AEC was about 10 t/h. Both ideal AECs and residual AECs under SE and NW type circulations had great diurnal variations with the maximum value appearing at 16:00, the maximum value of residual AEC exceeding 20 t/h.

Compared with the actual AEC under clean circulations, the actual AEC under polluted circulations was dramatically higher and close to ideal AEC so that the residual AEC fluctuated around zero. The average

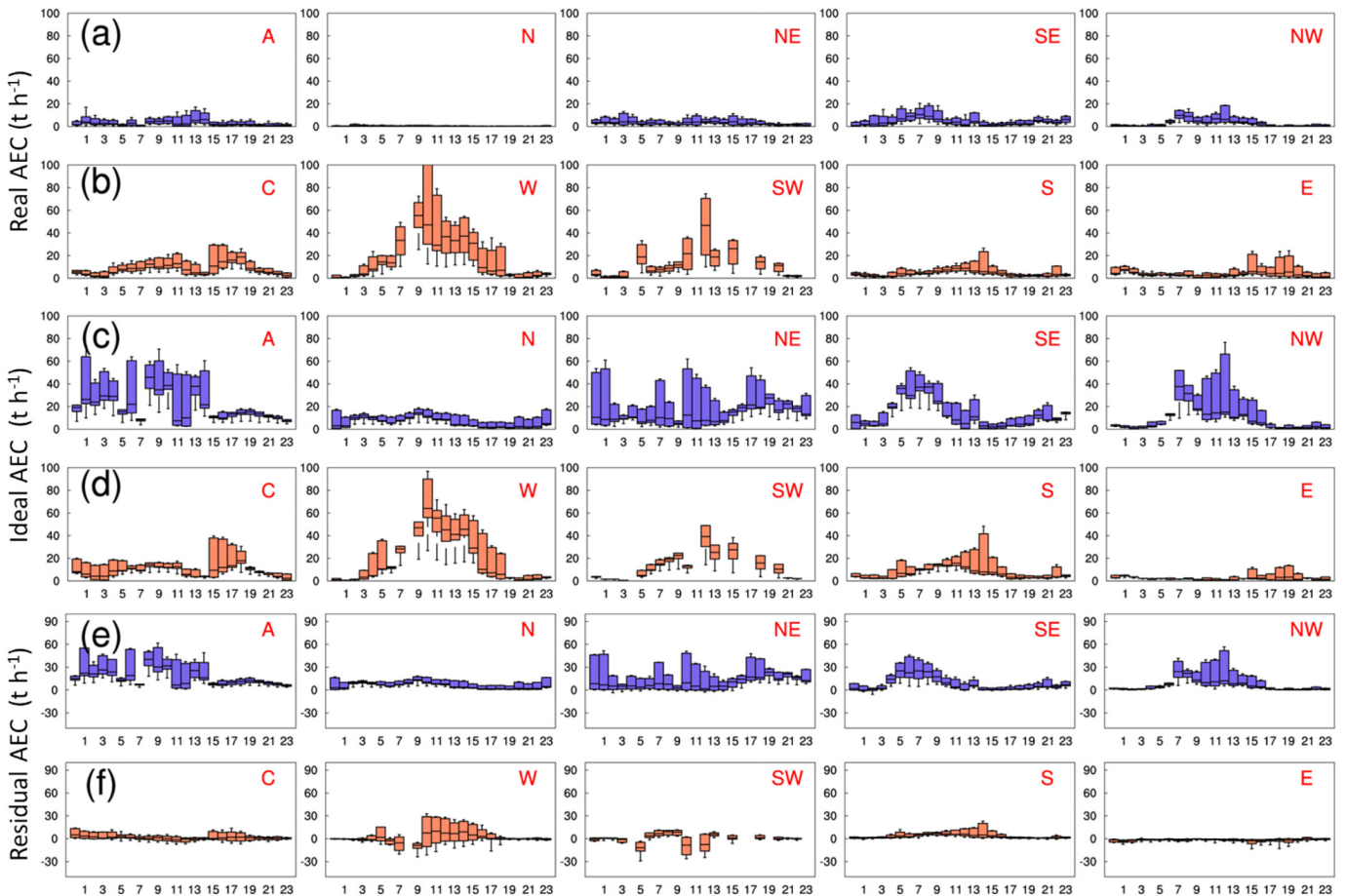


Fig. 7. The diurnal variation of real AEC (a, b), ideal AEC (c, d) and residual AEC (e, f) under different circulation patterns. Blue and red boxes represent clean and polluted circulation patterns, respectively. Clean types include anticyclonic (A), northerly (N), northeasterly (NE), southeasterly (SE) and northwesterly (NW) circulations. Polluted types include cyclonic (C), westerly (W), southwesterly (SW), southerly (S) and easterly (E) circulations.

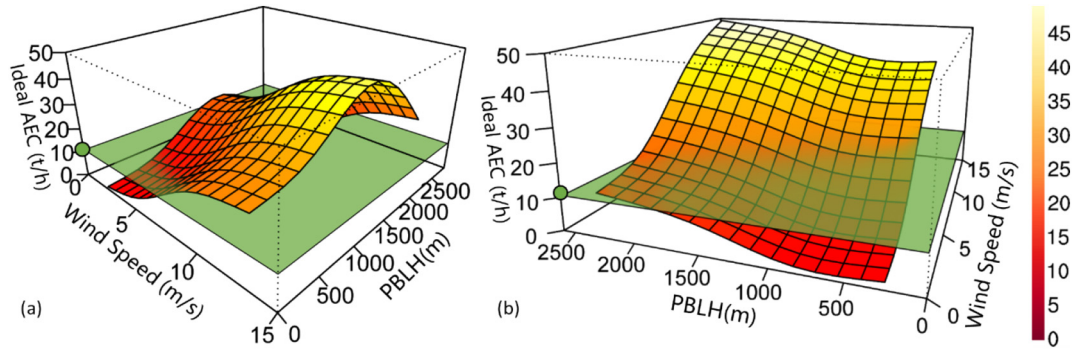


Fig. 8. The three-dimensional plot of the ideal AEC fitted by the planetary boundary layer height (PBLH) and horizontal wind speed calculated from the improved dynamic algorithm under polluted circulations (a) and clean circulations (b). The green dot represents AEC calculated by empirical constant values used in national standard.

actual AEC under C-type circulation gradually increased to 15 t/h during the daytime and decreased at night. The ideal AEC was larger than the actual AEC from 8:00 to 12:00 and then gradually smaller than the actual AEC. Therefore, the residual AEC changed from positive to negative, and the minimum is about -5 t/h . Negative residual AECs signified that the emission intensity has exceeded the air quality standard and the atmosphere has been overloaded for $\text{PM}_{2.5}$. The actual AEC and ideal AEC under W-type circulation showed remarkable daily variations, and the AEC had a wide range at fixed time (Fig. 7b, d). Both the maximum and the minimum of residual AEC, which ranged from -10 t/h to 50 t/h , appeared around 18:00 (Fig. 7f), indicating that the $\text{PM}_{2.5}$ concentration differed significantly in the afternoon between districts. The actual AECs under the background of SW, S, and E circulations were generally less than 15 t/h (Fig. 7b). The ideal AECs under SW and S type circulations were so close to the actual AEC that the residual AECs were slightly greater than zero (Fig. 7f), suggesting that the emission of pollutants basically kept in balance with atmospheric purifying under that meteorological conditions. The ideal AEC under E-type circulation was the smallest in the polluted circulations, which was smaller than the actual AEC in most time. Therefore, the residual AEC was less than zero and the minimum value was no less than -5 t/h .

The three-dimensional plot of the ideal AEC under polluted circulations and clean circulations are shown in Fig. 8. The PBL height represents the maximum vertical distance of diffusion of pollutants, and the wind speed represents the horizontal ventilation strength. The ideal AEC under polluted types increased with the PBL height when the PBL height was lower than 1500 m, and then decreased rapidly. Meanwhile, the ideal AEC also increased with the horizontal wind speed when the speed was lower than 6 m/s, and the increasing will be quite slow

when the velocity was larger than 6 m/s (Fig. 8a). It can be summarized that the ideal AEC under polluted types does not increase indefinitely with wind speed and PBL height, usually not exceed 40 t/h. This is because if the PBL height and wind speed continue to increase, it will gradually turn into a clean circulation type. By contrast, the ideal AEC under clean types was prominently larger than that of polluted types and increased with the PBL height and horizontal wind velocity continuously. The fastest increase of ideal AEC occurred when it was between 10 t/h and 30 t/h, and the maximum value reached about 50 t/h. When the wind speed was lower than 5 m/s and the PBL height was greater than 2500 m, the ideal AEC was about 10 t/h. However, when the wind speed was greater than 15 m/s, even if the PBL height was lower than 500 m, the ideal AEC was still greater than 35 t/h. This indicated that the contributions of horizontal advection on enlarging the environmental capacity are much higher than the vertical diffusion under clean circulations.

5. Conclusions

In this paper, the following improvements are made to derive the dynamic AEC for aerosols because the traditional A-value method is very subjective in view of the empirical coefficient A, and is only suitable for annual AEC of gaseous pollutants: The AEC was calculated with PBL observational data with high temporal resolution rather than a series of empirical fixed values. The time coefficient term is added to the algorithm to make it suitable for the hourly-scale dynamic AEC. And the single-box model was modified to multi-box model to make the AEC algorithm suitable for aerosol pollutants. Compared with traditional single box model (Fig. 9a), when the $\text{PM}_{2.5}$ concentration and horizontal

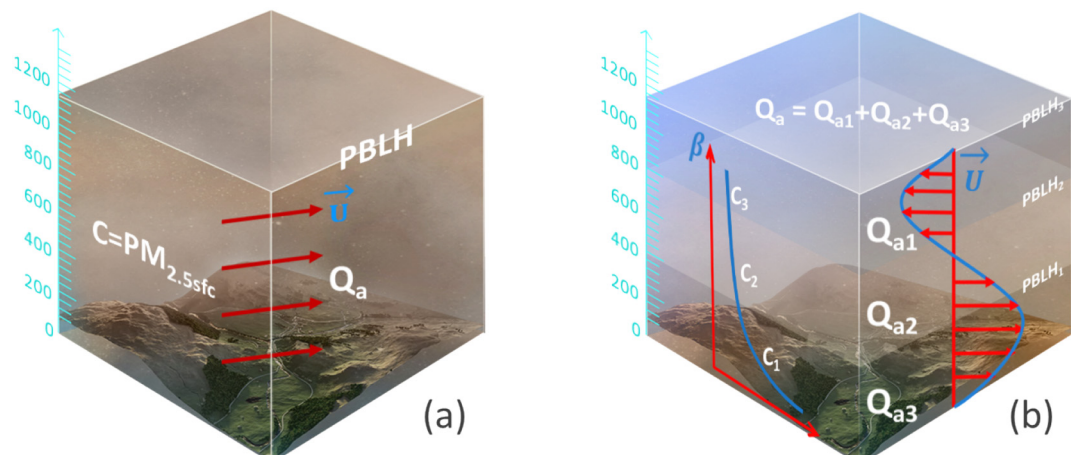


Fig. 9. A conceptual scheme of traditional A-value method based on single box model (a) and the improved dynamic method based on multi-box model (b).

winds change greatly vertically (Fig. 9b), the improvement of multi-box model is much more remarkable, such as A, NE and W type circulations. While the initial PM_{2.5} concentration, horizontal wind speed and PBL heights change greatly with time, the improvement by the time coefficient is much more conspicuous, such situation is consistent with most circulation patterns. The ideal AEC characterizes the maximum purification capacity of the atmosphere depending on meteorological conditions. The magnitude and sign of residual AEC indicate whether the atmosphere has been overloaded or has surplus capacity for PM_{2.5} and the emission should be reduced. Further applying of the circulation typing method to ideal AEC and residual AEC provides a reference for the practical prediction of AEC under different circulation background. In the current dynamic multi-box model, the influences of background concentration of PM_{2.5} in the upstream on AEC are not taken into consideration. The clean circulations are often accompanied by northerly airflow with a lower background concentration, and the advection will reduce the pollutant concentration in the control area. However, this effect will be attributed to the emissions in the original equation so that the actual AEC will be underestimated in clean circulation types. On the contrary, the actual AEC can be overestimated in polluted circulation types. These impacts on AEC should also be taken into account to optimize the algorithm and reduce the errors in future work.

CRediT authorship contribution statement

Yunyan Jiang: Methodology, Software, Visualization, Writing-Reviewing and Editing. **Jinyuan Xin:** Conceptualization, Writing guidance, Funding acquisition and Revising. **Zifa Wang and Yongli Tian:** Supervision. **Guqian Tang and Yuanzhe Ren:** Contribution to observation data and discussions of results. **Lin Wu, Xiaole Pan and Ying Wang:** Data Curation. **Danjie Jia and Yongjing Ma:** Investigation and Resources. **Lili Wang:** Polishing the article. All the authors have made substantial contributions to this article.

Declaration of competing interest

The authors declare that they have no known competing financial interests or personal relationships that could have appeared to influence the work reported in this paper.

Acknowledgments

This study was supported by the CAS Strategic Priority Research Program (XDA23020301), the major science and technology project of Inner Mongolia Autonomous Region (2020ZD0013), the National Natural Science Foundation of China (42061130215), and the Royal Society (NAF|R1|201354).

References

- An, X.Q., Chen, Y.C., Lü, S.H., 2004. Study on SO₂ atmospheric environment capacity in Lanzhou winter. *Plateau Meteorol.* 23 (1), 110–115 (in Chinese).
- An, X.Q., Zuo, H.C., Chen, L.J., 2007. Atmospheric environmental capacity of SO₂ in winter over Lanzhou in China: a case study. *Adv. Atmos. Sci.* 24 (4), 688–699.
- Chen, S., Zhang, X., Lin, J., Huang, J., Zhao, D., Yuan, T., Huang, K., Luo, Y., Jia, Z., Zang, Z., Qiu, Y.A., 2019. Fugitive road dust PM_{2.5} emissions and their potential health impacts. *Environ. Sci. Technol.* 53 (14), 8455–8465.
- Chen, L., Zhu, J., Liao, H., Yang, Y., Yue, X., 2020. Meteorological influences on PM_{2.5} and O₃ trends and associated health burden since China's clean air actions. *Sci. Total Environ.* 744, 140837.
- Dai, H., Zhu, J., Liao, H., Li, J., Liang, M., Yang, Y., Yue, X., 2021. Co-occurrence of ozone and PM_{2.5} pollution in the Yangtze River Delta over 2013–2019: Spatiotemporal distribution and meteorological conditions. *Atmos. Res.* 249, 105363.
- Gao, S., Li, S.B., Ma, Y., Li, G., Bo, X., Qu, J.B., Lei, T.T., Mao, N., Lu, R.J., Ren, H.L., 2021. Research on atmospheric environmental capacity accounting method based on classification of meteorological conditions. *China Environ. Sci.* 41 (2), 588–595 (in Chinese).
- GB 3095–2012. Ambient air quality standards. Ministry of Environmental Protection of the People's Republic of China (in Chinese).
- Han, Z., Zhou, B., Xu, Y., Wu, J., Shi, Y., 2017. Projected changes in haze pollution potential in China: an ensemble of regional climate model simulations. *Atmos. Chem. Phys.* 17 (16), 10109–10123.
- Hanna, S.R., Briggs, G.A., Hosker Jr., R.P., 1982. *Handbook on atmospheric diffusion (No. DOE/TIC-11223)*. National Oceanic and Atmospheric Administration, Oak Ridge, TN (USA). Atmospheric Turbulence and Diffusion Lab.
- Hao, J.M., Xu, J.Y., Wu, J., Ma, Q., 2017. A study of the atmospheric environmental capacity of Jingjinji and of the five northwestern provinces and autonomous regions in China. *Strateg. Stud. Chin. Acad. Eng.* 19 (4), 13–19 (in Chinese).
- Huang, X., Ding, A., Gao, J., Zheng, B., Zhou, D., Qi, X., Tang, R., Wang, J., Ren, C., Nie, W., Chi, X., 2021. Enhanced secondary pollution offset reduction of primary emissions during COVID-19 lockdown in China. *Natl. Sci. Rev.* 8 (2), nwaa137.
- Jenkinson, A.F., Collison, F.P., 1977. An initial climatology of gales over the North Sea. 62, 18.
- Jiang, Y., Xin, J., Wang, Y., Tang, G., Zhao, Y., Jia, D., Zhao, D., Wang, M., Dai, L., Wang, L., Wen, T., 2021a. The thermodynamic structures of the planetary boundary layer dominated by synoptic circulations and the regular effect on air pollution in Beijing. *Atmos. Chem. Phys.* 21 (8), 6111–6128.
- Jiang, Y., Xin, J., Zhao, D., Jia, D., Tang, G., Quan, J., Wang, M., Dai, L., 2021b. Analysis of differences between thermodynamic and material boundary layer structure: comparison of detection by ceilometer and microwave radiometer. *Atmos. Res.* 248, 105179.
- Lamb, H.H., Hh, L., 1972. British Isles weather types and a register of the daily sequence of circulation patterns, pp. 1861–1971.
- Lettau, H.H., 1970. Physical and meteorological basis for mathematical models of urban diffusion processes. 2–1.
- Li, L., Cheng, S.Y., Chen, D.S., Hao, L.B., Fu, H.L., 2010. A calculated methodology of atmospheric environmental capacity based on CMAQ and control strategy. *Environ. Sci. Technol.* 33 (8), 162–166.
- Li, M.H., Liao, C.H., Yang, L.L., Zeng, W.T., Tang, X.B., 2018. Capacity simulation method based on regional transfer matrix and PM_{2.5} concentration target constraint. *Environmental. Science* 39 (8), 3485–3491 (in Chinese).
- Liao, Z., Gao, M., Sun, J., Fan, S., 2017. The impact of synoptic circulation on air quality and pollution-related human health in the Yangtze River Delta region. *Sci. Total Environ.* 607, 838–846.
- Lin, J., Nielsen, C.P., Zhao, Y., Lei, Y., Liu, Y., McElroy, M.B., 2010. Recent changes in particulate air pollution over China observed from space and the ground: effectiveness of emission control. *Environ. Sci. Technol.* 44 (20), 7771–7776.
- Lu, C.J., Shi, X.F., 2008. Discussion on linear programming method for calculating atmosphere bearing capacity of an industrial park [J]. *Environ. Sci. Technol.* 31 (10), 142–144.
- Münkel, C., Eresmaa, N., Räsänen, J., Karppinen, A., 2007. Retrieval of mixing height and dust concentration with lidar ceilometer. *Bound.-Layer Meteorol.* 124 (1), 117–128.
- Ou, Y.X.G., 2008. Research on the a value amending algorithm for AP value method in EPC calculation. *Res. Environ. Sci.* 21 (1), 37–40 (in Chinese).
- Pleijel, H., Grundström, M., Karlsson, G.P., Karlsson, P.E., Chen, D., 2016. A method to assess the inter-annual weather-dependent variability in air pollution concentration and deposition based on weather typing. *Atmos. Environ.* 126, 200–210.
- Pope, R.J., Butt, E.W., Chipperfield, M.P., Doherty, R.M., Fenech, S., Schmidt, A., Arnold, S.R., Savage, N.H., 2016. The impact of synoptic weather on UK surface ozone and implications for premature mortality. *Environ. Res. Lett.* 11 (12), 124004.
- Qian, Y., Wang, Q., 2011. An integrated method of atmospheric environmental capacity estimation for large-scale region. *China Environ. Sci.* 31 (3), 504–509 (in Chinese).
- Russo, A., Trigo, R.M., Martins, H., Mendes, M.T., 2014. NO₂, PM10 and O₃ urban concentrations and its association with circulation weather types in Portugal. *Atmos. Environ.* 89, 768–785.
- Steyn, D.G., Baldi, M., Hoff, R.M., 1999. The detection of mixed layer depth and entrainment zone thickness from lidar backscatter profiles. *J. Atmos. Ocean. Technol.* 16, 953–959.
- Tang, G., Zhu, X., Hu, B., Xin, J., Wang, L., Münkel, C., Mao, G., Wang, Y., 2015. Impact of emission controls on air quality in Beijing during APEC 2014: lidar ceilometer observations. *Atmos. Chem. Phys.* 15, 12667–12680. <https://doi.org/10.5194/acp-15-12667-2015>.
- Tang, G., Zhang, J., Zhu, X., Song, T., Münkel, C., Hu, B., Schäfer, K., Liu, Z., Zhang, J., Wang, L., Xin, J., Suppan, P., Wang, Y., 2016. Mixing layer height and its implications for air pollution over Beijing, China. *Atmos. Chem. Phys.* 16, 2459–2475. <https://doi.org/10.5194/acp-16-2459-2016>.
- Trigo, R.M., DaCamara, C.C., 2000. Circulation weather types and their influence on the precipitation regime in Portugal. *Int. J. Climatol.* 20, 1559–1581.
- Wang, J.N., Pan, X.Z., 2005. Application of linear programming in the allocation of environmental capacity resources. *Environ. Sci.* 26 (6), 195–198 (in Chinese).
- Wang, Q.G., Wu, Y.M., Li, Z.K., 1997. A improved A-P method. *Acta Sci. Circumst.* 17 (3), 278–283 (in Chinese).
- Wang, S., Gao, J., Zhang, Y., Zhang, J., Cha, F., Wang, T., Ren, C., Wang, W., 2014. Impact of emission control on regional air quality: an observational study of air pollutants before, during and after the Beijing olympic games. *J. Environ. Sci.* 26 (1), 175–180.
- Wang, H.J., Wang, Y.C., Ni, C.J., 2015. Calculating the seasonal atmospheric environmental capacity in Chengdu based on modified a value method. *Environ. Sustain. Dev.* 40 (3), 71–74 (in Chinese).
- Wen, J.Y., Wang, Z.S., Hu, Y., Li, Z., Li, Y., 2013. Application of interval-fuzzy linear programming for Total amount control optimization model on regional atmospheric pollutants. *Appl. Mech. Mater.* 316–317, 493–496.
- Xiao, Y., Mao, X.Q., Ma, G.H., Li, Z., 2008. Atmospheric environmental capacity study based on ADMS model and linear programming. *Res. Environ. Sci.* 21 (3), 13–16 (in Chinese).
- Xu, D., Li, Z., 1993. The relationship between A-P value method and multiple sources dispersion model in the Total quantity control of air pollutants emission in urban area. *Sci. Meteorol. Sin.* 13 (2), 146–154 (in Chinese).
- Xu, D., Zhu, R., 1989. A study on the distribution of ventilation and rainout capacity in mainland China. *China Environ. Sci.* 9, 367–374 (in Chinese).

- Xu, D., Zhu, R., Pan, Z., 1990. The studies on standard of emission of SO₂ and dispersion model in cities. *China Environ. Sci.* 10 (4), 309–313 (in Chinese).
- Xu, D., Wang, Y., Zhu, R., 2016. The atmospheric environmental capacity coefficient cumulative frequency curve fitting and its application. *China Environ. Sci.* 36 (10), 2913–2922 (in Chinese).
- Xu, D., Wang, Y., Zhu, R., 2018a. Atmospheric environmental capacity and urban atmospheric load in mainland China. *Sci. China Earth Sci.* 61 (1), 33–46 (in Chinese).
- Xu, Y.L., Xue, W.B., Wang, J.N., Lei, Y., Ye, Z.L., Ren, Z.H., 2018b. Development and prospect of atmospheric environment capacity theory and accounting method. *Res. Environ. Sci.* 31 (11), 1835–1840 (in Chinese).
- Xu, Y.L., Xue, W.B., Lei, Y., 2019. Impact of meteorological conditions and emission change on PM2.5 pollution in China. *China Environ. Sci.* 39 (11), 4546–4551 (in Chinese).
- Xue, W., Wang, J., Niu, H., Yang, J., Han, B., Lei, Y., Chen, H., Jiang, C., 2013a. Assessment of air quality improvement effect under the national total emission control program during the twelfth national five-year plan in China. *Atmos. Environ.* 68, 74–81.
- Xue, W.B., Wang, J.N., Yang, J.T., Lei, Y., Wang, Y.M., Chen, X., 2013b. Domestic and foreign research progress of air quality model. *Environ. Sustain. Dev.* 3, 14–20 (in Chinese).
- Xue, W., Fu, F., Wang, J., He, K., Lei, Y., Yang, J., Wang, S., Hang, B., 2014a. Modeling study on atmospheric environmental capacity of major pollutants constrained by PM2.5 compliance of Chinese cities. *China Environ. Sci.* 34 (10), 2490–2496 (in Chinese).
- Xue, W., Fu, F., Wang, J., Tang, G., Lei, Y., Yang, J., Wang, Y., 2014b. Numerical study on the characteristics of regional transport of PM2.5 in China. *China Environ. Sci.* 34 (6), 1361–1368 (in Chinese).
- Yang, Q.J., Zhao, T.L., Zheng, X.B., 2019. Assessments of the differences of atmospheric environmental capacity between strong and weak Asian monsoon years in Mengzi. *China Environ. Sci.* 39 (10), 4054–4064 (in Chinese).
- Yuan, J., Tian, W., Cheng, C., Yu, J., 1996. Study of SO₂ Total emission control over Xigu District, Lanzhou. *J. Lanzhou Univ. Nat. Sci.* 32 (4), 170–176 (in Chinese).